Progress In Electromagnetics Research M, Vol. 81, 1–11, 2019

Interference of Radar Detection of Drones by Birds

Jiangkun Gong[1, *], Jun Yan[1], Deren Li[1], Deyong Kong[2], and Huiping Hu[3]

Abstract—Recently, consumer drones have encroached upon airports and pose a potential threat to aviation safety. Radar is an effective remote sensing tool to detect and track flying drones. Radar echoes from flying birds are assumed to be clutters when a radar is detecting drones. Yet, few studies have reported how radar echoes from flying birds interfere with the detection of drones, how similar radar cross section (RCS) and flight feature of birds and drones are, and why the flying birds cause trouble when radar identifies signals from the drone. In this study, we collected 3900×256 of Ku-band radar echoes of flying birds and consumer drones. The targets consist of a pigeon, a crane, waterfowl, and a DJI Phantom 3 Vision drone. We compared the maximum detectable range of birds and drones, the time series and the Doppler spectrum of radar echoes from the birds and the drone, considering oncoming and outgoing radar data with respect to radar location. The statistical results indicate that flying birds have similar RCS, same velocity range, similar signal fluctuation, and approximate signal amplitude. Our results of radar automatic target recognition (ATR) illuminate that the identification probability of airborne drones will be lower due to the interference of the radar signal by flying birds. Above all, these facts confirm that flying birds are the main cause of interference when a radar is detecting and identifying airborne drones.

1. INTRODUCTION

The growing popularity of drones among consumers and commercial users provides both benefits and threats. One of the threats is the collision of drones and manned aircraft [1]. Investigation of the damage posed by drones on aircraft shows that drones pose a greater level of threat than what existing regulations allow, as well as more serious damage than that of flying birds [2, 3]. It has been reported that a majority of the total incidents involving drones and aircraft took place within five miles of an airport, which is likewise prohibited airspace for all drones, regardless of the altitude at which they are flying [4]. Most of the drones identified in reports are multirotors (e.g., quadcopters, hexacopters). Therefore, there is an urgent need to detect multirotor drones in order to adopting countermeasures. Yet, the primary mission is detection and identification, which are the preconditions of countermeasures.

Radar is the most powerful tool that can remotely sense flying drones in the vicinity of airports. Compared with optical and infrared detection, radar can extend observational capabilities to around-the-clock operations and expand spatial coverage in both distance and altitude, despite interference by bad weather such as rain, fog, and darkness, when vision is impaired [5]. Air surveillance radars (ASRs) are not fit for detecting drones at low altitude because the mission of ASR focuses on searching for aircraft that have a large radar cross section (RCS) in the sky, not at low altitude [6, 7]. Besides, detection of drones with high range resolution radar profiles (HRRPs) is problematic because sub-centimeter resolution is needed to capture the longitudinal structure of targets less than 100 cm in length [8, 9]. Therefore, most radar systems being used to detect and identify birds and drones have a low range profile.

Received 5 February 2019, Accepted 22 March 2019, Scheduled 22 April 2019

* Corresponding author: Jiangkun Gong (gjk@whu.edu.cn).

[1] State Key Laboratory of Information Engineering in Surveying, Mapping and Remote Sense, Wuhan University, China. [2] School of Information and Communication Engineering, Hubei University of Economics, China. [3] Wuhan Geomatics Institute, China.

Flying birds are supposed to be the major jamming targets for detecting drones. Flying birds are the masters of the sky, and bird strike hazards are the principal threat to the aviation industry [10]. For a long time ago, radar echoes from birds were called "angel echoes" because of its flickering characteristic [11, 12]. There is considerable overlap between bird tracks and those of man-made targets, especially light aircraft (Nowdays, they are drones.) and helicopters [13]. The measured bird flight speeds span varies from several m/s up to a maximum of 43 m/s, and the bird altitude during flight is blow 2000 m for the vast majority of migrating birds around Europe, while the bird density can be 10^5 to 10^6 birds within 50 km of a ship-borne surveillance radar [13]. A typical customer drone is DJI Phantom. It weighs several kg and a top speed of 16 m/s [6]. Despite the fact that the maximum flight height of a drone is 6000 m, the general altitude at which drones are allowed to fly is several hundreds of meters [4]. The researches on the differentiation between flying birds and small drones by radar are relatively new. Yet, the common view is that birds become the major jamming of radar detecting drones because of the similarity in RCS [14, 15], motion pattern [9, 16, 17], and even similar micro-Doppler features [18]. Moreover, Ritchie et al. reported that various birds will interfere with micro-drones in comparable signature within the time domain and similar RCS values, and the discrimination between birds and drones is needed to avoid significant false alarm rates [19]. When collecting radar data from a drone with L-band multibeam staring radar, Jahangir et al. usually obtain unexpected radar echoes that almost certainly are birds in multiple scenarios [6]. Obviously, birds can jam the detection of drones. Many researches have involved discussion about classification between birds and drones [8, 15, 19, 20]. Yet, several questions remain unanswered before we investigate the potential methods of classification between birds and drones. Are flying birds the major source of clutter for radar detecting airborne drones? How much similar do their radar echoes look like, as for RCS, time series, spectrum, flight feature or micro-Doppler features? How much do radar echoes from flying birds affect the detection of drones? What are the difficulties presented by the birds' echoes for classifying drones from flying birds? Those questions have been inadequately investigated by researchers.

For the first time, in this paper, we argue that radar echoes from flying birds are the major source of clutter when radar detects airborne drones by presenting some experimental results, including comparisons of the maximum detectable range of drones and birds, statistics of both time series and Doppler spectrums of radar echoes from drones and birds, and observation recognition results. We prudently design experiments to gather radar data from flying birds and drones. We introduce the scattering regions theory into the analysis of radar data. We discuss the differences and similarities between the radar signals of birds and that of drones, including the distribution of scattering centers, the signal amplitude, the fluctuation of signal amplitude, and Doppler velocity. At last, we present statistical results of automatic target recognition (ATR) to demonstrate the disturbance of flying birds on identifying flying drones

2. MATERIALS AND METHODS

Before discussing the interference of radar detection of drones by birds, radar bands should be analyzed because they affect radar scattering characteristics completely. Radar scattering characteristics primely depend on the ratio of the radar wavelength to the target size. There are three scattering regions used to describe the scattering mechanism: the Rayleigh region, Mie region (resonance region) [21], and optical region [22, 23]. The RCS is the most common scattering characteristic. It is used to measure a target's efficiency for scattering radiation back to its source, or in other words, RCS is the size of the target as "seen" by the radar. In the Rayleigh region, where the target size is much smaller than the wavelength, and the RCS of the flying target increases linearly with the incident frequency, meaning that we can barely estimate the size of the target. In the Mie region, when the target's size is like that of the wavelength, the resonance of the target at the incident frequency makes its RCS fluctuate over time. Multiple peaks, i.e., "scattering poles" in the spectrum represent varying material compositions of the target. In the optical region, when the target size is much greater than the wavelength, scattering occurs at certain points on the target. Those certain points are scattering centers. RCS of the target fluctuates because it takes into consideration the shape and attitude of the target. In brief, any attempts to describe target shape will fail in the Rayleigh region and Mie region, but not in the optical region.

In order to improve the detection probability of small targets (i.e., birds, drones) with low RCS

value, current radar systems choose those bands (mainly S-band and L-band) [24] that have a wavelength similar to that of the size of birds and drones, in which the scattering field will fall into the Mie region where the target echo intensity is enhanced because of the resonance effect [25], and the detection range of a target is increased. Nevertheless, when radar data come from the Mie region, the target shape cannot be characterized by radar data and used for classifying birds and drones. However, we choose radar band (i.e., Ku-band) in the optical region because we try to describe target shape to classify birds and drones based on the difference of their shapes.

The Ku-band pulse Doppler phased-array radar is equipped with an automatic target recognition (ATR) function. The discussion on the algorithm of this ATR function goes beyond the scope of this article. The radar can identify radar echoes from people, ground vehicles, drones, and birds among complex scenes in the field of the radar beam. It is capable of obtaining large time-bandwidth results, achieving long detection ranges and medium-range resolution simultaneously with linear frequency modulation technology. The working band is Ku (12–18 GHz), and the typical wavelength is 2 cm. The range resolution is 15 m. Its peak power is 384 W when all T/R subunits are working. Its pulse repetition frequency (PRF) is 6 kHz. The sample data are output from a signal processing unit in 32-bit floating point format. The coherent processing interval (CPI) is 30 ms. The number of sampling data points in one CPI is 256. All the parameters were calibrated to guarantee that the radar was working correctly.

The whole experiments were performed at an area of the Yellow River wetland bird protection area in China. The test environment includes roads, rivers, farmlands, and forests. Moving targets include vehicles, people, sheep, and birds. The pigeon has the mass of 0.35 kg. It was tethered with a 100-m-long cotton rope that was invisible to the radar. The pigeon could fly for a short distance in the air but could not get away. The drone used in this experiment is a Phantom 3 Vision (DJI, China). It is classified as a quadcopter with the propellers having a tractor configuration. Both its body and propellers are mainly composed of plastic. The four individual rotors are composed of carbon fiber and plastic. The mass of this drone is 1.280 kg. Its maximum horizontal flight speed is 16 m/h. The maximum rotary speed of its rotor blades is 150°/s. Its maximum flight height is 6000 m. It can fly for a total of 23 min.

In order to provide comparisons of radar echoes from birds and drones, we conducted several types of tests to collect radar data. First, we evaluated the maximum detectable range of the pigeon and the drone. According to the radar equation [22], the radar detection range of a specified target is proportional to the fourth root of its RCS, if the radar system is specified. If the maximum detectable ranges ($R_{\max}$) of the pigeon and the drone are similar, their RCS values are approximate too. The radar was put on the top of a plateau and scanned the test zone to detect the flying pigeon and drone about 12 km away. The $R_{\max}$ is calculated by [22],

$$R_{\max}^4 = \frac{P_t G A_e \sigma}{(4\pi)^2 k T_0 B_n F_n S N R_{\min}} \tag{1}$$

where P_t = transmit power, G = transmitting gain, A_e = effective area of the receiving antenna, B_n = noise bandwidth of the receiver, σ = radar cross section of the target, T_0 = a standard temperature, which the IEEE defines as 290 K, F_n = noise figure, $\mathrm{SNR}_{\min}$ = the minimum signaltonoise ratio (SNR). Second, we collected radar echoes from birds and drones at specific range gates. In order to eliminate the potential clutters, we select a test area, where the drone and the pigeon are flying, at the mean time, our tester observes whether there are extra moving targets or not and informs the radar operator the situation in time. The radar was placed on a road at the foot of a plateau. From there, the test area was scanned horizontally. The detection range of the drone is 1.2 km. The drone was flying away from the radar and then flying back toward the radar. The radar was in scanning mode, and radar data in the range gate where the drone was flying were extracted. Under the same conditions, we recorded radar signals from the flying pigeon at the range of 2.4 km. It was flying in a circle. With those radar data at the same range, we can analyse the time-series of radar echoes, as well as their Doppler spectrums. Note that, there is not a general direction of pigeon flight recorded, because we find that it is quite difficult to control the direction of the pigeon flight. The scattering centers distribution images are obtained via

a continuous wavelet transform (CWT). The CWT is described as

$$X_w(a,b) = \frac{1}{|a|^{1/2}} \int_{-\infty}^{\infty} x(t)\bar{\psi}\left(\frac{t-b}{a}\right) dt \tag{2}$$

where a = scale, b = translational values, $x(t)$ = time series of radar data in one range gate. The name of the wavelet is Daubechies vavelets. We process radar data with Matlab to plot the scaled images of the scalogram. Third, we try to evaluate the jamming level posed by birds, when the radar is detecting a drone. Thanks to the ATR function of our radar system in this experiment, we can report the statistics of detection cases. We used radar to search for a fixed area, where the drone was flying freely. The radar operator did not know the precise position of drones. In this area, our human observation distinguish some bird species, including cranes and other waterfowls. We recorded the recognition results output from the radar ATR processing system. The frame whole number of radar echoes from flying birds is 2900, while that from flying drones is 1000. Since the number of sampling data points in one CPI or sampling frame is 256, the total radar data of birds and drones are 2900×256, 1000×256.

3. RESULTS

Since we used the Ku-band radar, our radar data fell into the optical region. Note that the target size is the projection area on the cross-section perpendicular to the direction of the site of the radar. When the target is a sphere, the "target size" is equal to the cross-sectional area. Common radar bands utilized for detecting birds and drones are the L-, S-, X-, and Ku-bands. Therefore, the scattering field in the Mie region has something to do with L- and S-bands. In this situation, both birds and drones are different size spheres in the view of the radar, but are composed of different materials. A flying bird may be a sphere with water, blood, and flesh, whereas in the case of an airborne drone, the sphere may be composed of carbon fiber, plastic, and metal. Scattering poles in the spectrum can refer to the material composition of the target. Yet, how to describe the relationship between distribution of the scattering poles and material composition is still under exploration. When radar data of the X- and Ku-bands are in the optical region, the scattering centers are utilized to describe the interaction between the electromagnetic wave and the target. Figs. 1(a) and (b) show the scattering centers of the pigeon and the drone, respectively. Those time-frequency distribution diagrams are obtained after transforming the original radar data with continuous wavelet transform (CWT). Highlight areas represent structures that reflect strong backscattering power, namely scattering centers of a target. If the target is a bird, scattering centers are bird beak, wings, body, and claws. For a drone, there are blades, motors, airframe, and the load. Besides, the comparison of distribution patterns in Figs. 1(a) & (b) indicates that the scattering distribution of a drone seems more orderly than that of a bird. In other words, a drone looks more like a sphere object in radar eyes than a bird. Actually, this interesting phenomenon is in accordance with human vision since a drone is more symmetrical than a bird, morphologically.

The maximum detectable ranges of the pigeon and drone are 12 km and 11 km, when the detection probability is above 95%. Since we use the same radar to measure the pigeon and drone at the same area, RCS values can be treated under the same measurement situation. Those results indicate that the pigeon and drone have a similar RCS value. Fig. 1(c) shows a radar image on radar B-scope, when the pigeon was flying at the range of 10.4 km. We can also note lots of clutters in this area, shown as the green and red dots. Some of the clutters are wild birds flying in the air. Despite the fact that this is a radar image of the pigeon, a similar situation also appears when radar detects the drone. From this radar image, we can image how much the bird influences the detection of drones. Overall, the time-series of those radar echoes, as well as their Doppler spectra, are similar. Typical radar echoes from the pigeon and drone are presented in Fig. 2. Doppler spectra are obtained by calculating the fast Fourier transform (FFT) on the time-series of radar signals. Signal fluctuations of the time-series exist in both the radar echoes from the bird and drone, no matter in which direction the object is flying. Despite the fact that it is not broadly apparent, we can observe that the spectral peak envelope of the drone is narrower and sharper than that of the bird. Additionally, there are bifurcations surrounding the main spectral peak of the bird, while that of the drone does not have any bifurcations. Another difference is the signal fluctuation. It is the fluctuation of the bird's signal a bit more violent than that

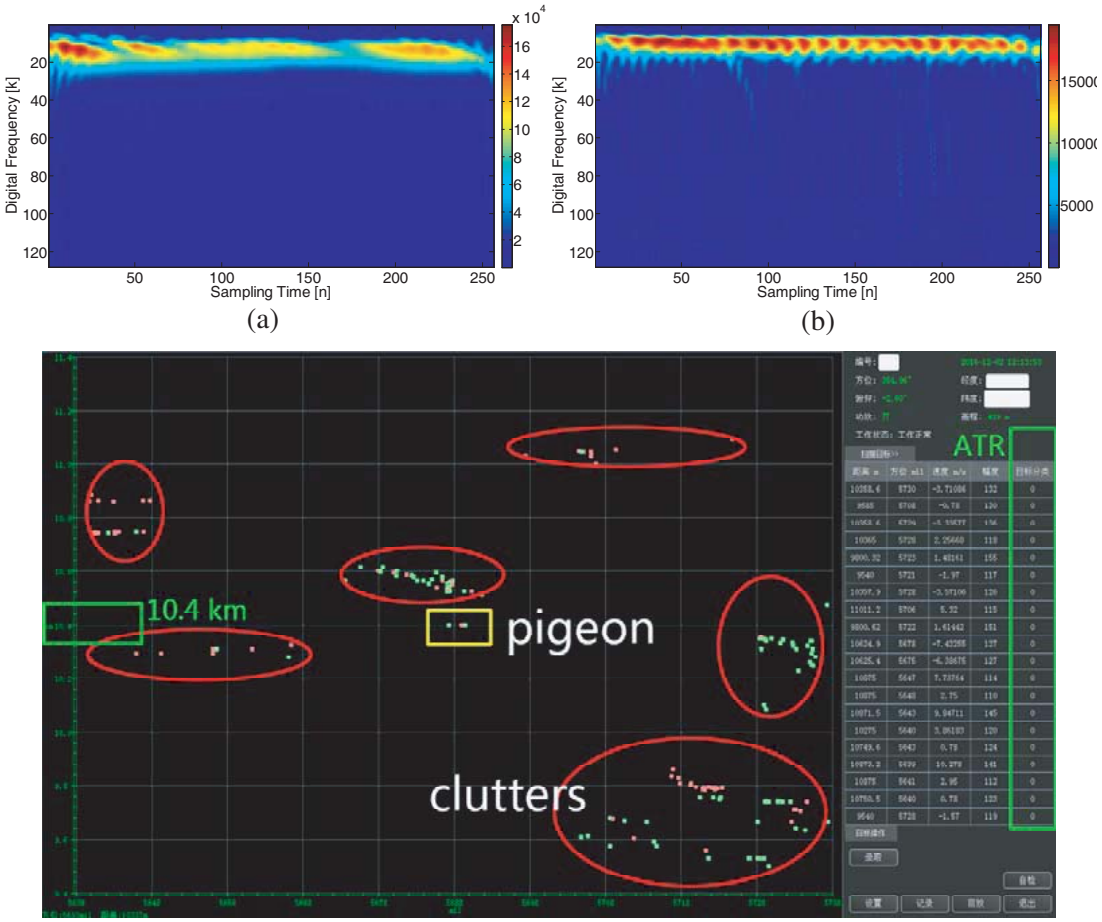

Figure 1. (a) Typical radar image of a bird; this is a pigeon. In the optical region, a target is treated as a distributed object in radar eyes, and scattering centers can describe the electromagnetic scattering between a target and radar wave. The heightened red regions are scattering centers of the bird. Scatteringcenters of a bird include bird beak, body, wings, legs and claws et. al. The observed pattern in the joint time-frequency distribution results from continuous wavelet transform (CWT). The bright red areas represent the strong received power. In the time-frequency plot produced by CWT, we can know when and where the scattering field happen. In other words, we can observe distribution pattern of scattering centers of a target. (b) Typical radar image of a drone; it is a DJI Phantom 3 Vision. The heightened red regions are scattering centers of the drone. The main scattering centers of a drone are blades, motors, airframe and the load. The distribution seems more orderly than that of Fig. 1(a). (c) This is a radar image of B-scope. The red dot and green dots in the yellow quadratic box show the trajectory of a flying pigeon. The range resolution is 15 m. As shown in the vertical axis, the range is 10.4 km, which can be longer than 12 km when the detection probability is above 95%. The green dots show outgoing objects moving away from the radar, while the red ones represent objects moving towards the radar. Those dots in the red oval boxes are clutters. Some of the clutters are wild birds flying in the air. The green quadratic boxes in the left of figure describes the detection range of 10.4 km. The data in the right green quadratic boxes are recognition results.

of the drone, especially comparing the signals of different flight directions. Yet, this difference does not exist in all radar data, meaning that there is difference in signal fluctuation, but it is not so stable.

No fundamental wingbeat frequency is found from radar echoes of flying birds. Due to the contraction and dilation during a wingbeat cycle of birds flying through the radar beam, the timing waveforms will variate correlated with the sequence of flapping and pausing phases of a bird, thus

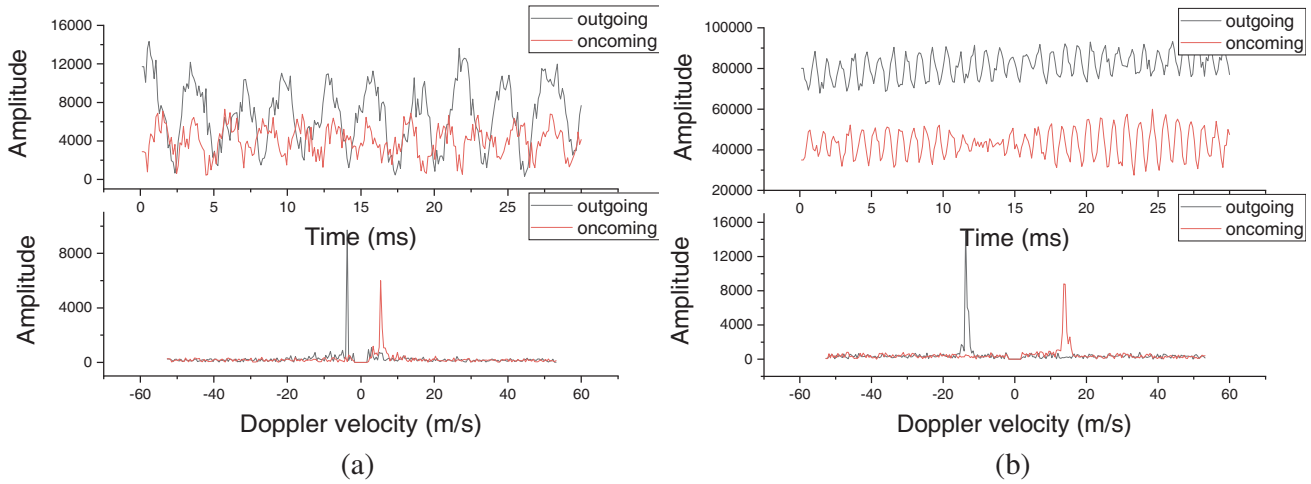

Figure 2. (a) Typical radar echoes from a drone flying away from the radar. (b) Typical radar echoes from a bird and its Doppler velocities. The drone is a DJI Phantom 3 Vision. The detection range of the drone is 1.2 km. The bird is a wild bird, detected at the range of 2.4 km from the radar location. The target's movement direction is judged by the positive and negative polarity of the Doppler spectral peak in the spectrum. There are 256 sampling points in one CPI of 30 ms. For most situations, both radar echoes from birds and drones are alike in either time-domain or spectra. Neither signal fluctuation nor Doppler velocity contribute much in distinguishing radar echoes from birds and drones, whether the object is flying away from the radar or not.

these "echo signatures" are, therefore, a means to recognize wingbeat frequencies, and then to distinguish between large and small birds, or between birds and man-made targets (here, drones). Bruderer et al. recognized wing-beat characteristics of birds recorded with tracking radar and cine camera, and categorized birds into passerine-like birds and geese-like birds [26]. Nevertheless, in practice, unambiguous wing flapping patterns can be difficult to detect [27]. Ireland and Williams showed that 40% of the tracks of birds were considered to be having irregular amplitude modulation [28]. Our observation also confirms that this periodic amplitude modulation posed by flapping is too ambiguous to be the difference between the radar echoes from flying drones and birds. Since the observation of wingbeat frequency is also related to sample time, our sampling time of one CPI (i.e., 30 ms) could be too short to record the cyclic amplitude variations modulated by wingbeats. Besides, we find that it is quite difficult to control the direction of the pigeon, even it is a cooperative target. In practice, a radar system records nearly impossibly a general direction of a bird flight. Radar data of a randomly flying bird are more common. Therefore, the observation of a periodic amplitude modulation posed by bird flapping is rare.

Generally, the RCS of a bird is thought to be smaller than that of a consumer-grade drone. Measurements of birds RCS values have been reviewed for many years. Experiments of Blacksmith and Mack show considerable RCS values of a duck and a chicken in the range of −9.5 to −13.5 dBsm with electromagnetic wave frequency of 400 MHz [29]. RCS values of three birds — grackle, sparrow, and pigeon tested by X-band radar — are present as −27.8 dBsm, −37.2 dBsm, and −28.2 dBsm, while for S-band radar, they are −25.7 dBsm, −28.2 dBsm, and −20.9 dBsm [30]. Vaughn refers to a sparrow having an RCS of −40 dBsm [31]. O'Neal n et al. provided a mean RCS the same as dabbling ducks (−19.4 dBsm) with a portable X-band radar [32]. Torvik et al. stated a medium sized bird with RCS of −25 dBsm [33]. They also quote "absolute numbers are not publicly available, but open information suggests that RCS values of the same order as of birds should be expected. This means that air surveillance radar designed to detect and track low RCS targets also will detect most birds in the area of potential targets" [34]. In 2016, Urmy and Warren pointed that mean tern RCS was estimated as −28 dBsm @ x-band [35]. Van Doren and Horton built a continental system for forecasting bird migration based on the assumption that a RCS per migratory medium sized bird of −29.6 dBsm [36]. The U.S. Federal Aviation Administration reported that the standard object detection of an avian

radar system is 2 km, while the standard object is a Standard Avian Target (SAT), which has the crow physical feathers with a mass of 0.5 kg and an RCS of −16 dBsm [24].

Recently, the researches on analysis of RCS values have propagated. Mean RCS values for carbon fiber and metalized blades of a drone at S-band are about −18 dBsm [37]. The authors showed that the RCS values of the entire UAV from measurements agreed with that from simulation, and their floating range is in −40 to −10 dBsm [17]. The measured main value of the RCS of a SYMA quadcopter was −15 dBsm at X-band, and the main RCS of a Airvision quadcopter was −5.6 dBsm [38]. Farlik et al. brought results of the series of RCS values with a DJI Phantom 2 Vision at X-band [39]. The mean RCS value of a typical quadcopter (i.e., DJI Phantom) is reported as −13 dBsm at W-band [40]. However, our experiment cannot support this claim. Fig. 3(a) exhibits the comparison of radar signals in intensity from a bird and a drone. The radar data in each frame are 256 sampling points. They are sampled in the range gate where the target is identified. We get the mean amplitude of the 256 radar echoes, and then we get one value in this frame. The total number of sampling frames is 100. The statistics show that the signal amplitude of a 0.35-kg bird is larger than that of a drone or at least not smaller than that of a drone. Note that the range of the bird is 2.4 km away from the radar, while the measured range of the drone is only 1.2 km. If they are detected at the same range of 2.4 km, the signal amplitude of the drone will be much lower than that of Fig. 3(a), and then the signal amplitude of the pigeon will be far more important than that of the drone. Our maximum detectable range of the pigeon and drone at 12 km and 11 km (Fig. 1(c)) also indicate that RCS of a 0.35-kg bird is larger than that of a drone. Those facts prove the usual idea that the RCS of a bird is less than a drone is not correct. At least, they may have a comparable RCS value. In addition to the parallel signal amplitude, their Doppler velocities are about the same as well. Fig. 3(b) shows the comparison of the Doppler

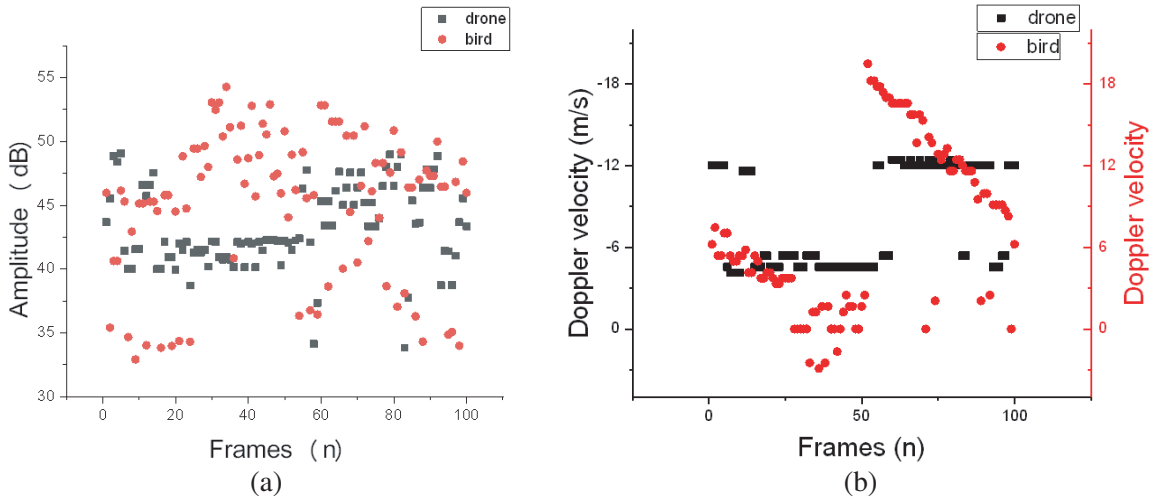

Figure 3. (a) Comparison of radar signal intensity from a bird and a drone. These are signal amplitude fluctuations of 100 frames. The vertical axis is the mean amplitude of signals in one frame. The horizontal axis is the frame serial number. The red signals are radar echoes from a pigeon, met in the 2.4 km from the radar, while the blue is signals of a drone at the distance of 1.2 km from the radar. The result indicates that bird radar cross section is more important than a drone. RCS does not represent a robust recognition feature for classifying birds and drones, since bird's RCS value is at the same level as that of a drone. (b) Comparison of Doppler velocity from a bird and a drone. These are Doppler velocities of birds and made in 100 frames. The vertical axis are Doppler velocities in one frame. The horizontal axis is the frame serial number. The red signals are radar echoes from a pigeon, met in the 2.4 km from the radar, while the blue is signals of a drone at the distance of 1.2 km from the radar. The velocities fluctuation of the bird is more vicious than that of the drone. Sometimes, red Doppler velocities are much greater than 15 m/s, which are due to wingbeat motion over than bird body movement. This indicates that Doppler velocity is simply not robust recognition feature for classifying birds and drones.

velocities between the bird and drone. Every point of Dopper velocity is derived from the spectrum in every sampling frame. A bird can fly agilely. Thus, its Doppler velocities change abruptly. On the contrary, the drone is flying much more steadily; thereby, its distribution of velocities is much smoother. In addition, sometimes the Doppler velocity of the bird comes from the flapping motion more than the body movement, which will exacerbate the fluctuation of the velocity.

The same velocity range, similar signal fluctuation, comparable signal amplitude, and common flight sky-area make flying birds a major disturbance when radar detects an airborne drone. Fig. 4 is the recognition of detecting the flying drones. On the test day, the drone was flying freely in the test area. The radar scanned this fixed area. When a target was detected, its radar data were recorded. Basically, radar data in the selected range gate were recorded. Sometimes, the drone was flying out of the range gate. In this area, there were some flying wild birds, including ducks, cranes, and other waterfowl, which were supported by human observation. These objects would be detected by the radar and appear on the radar display. Those birds will fly into the selected range gate. In this case, the ATR subsystem will identify the bird target in this range gate. The fundamental rule is that there can be only one target output in one range gate, and when both a bird and a drone are in the same gate, the ATR subsystem outputs the bird target. In brief, the interference of bird's echoes will lower the identification probability for identifying radar echoes from the drones, as shown in Fig. 4. The recognition results indicate that radar echoes from flying birds are the major source of clutter.

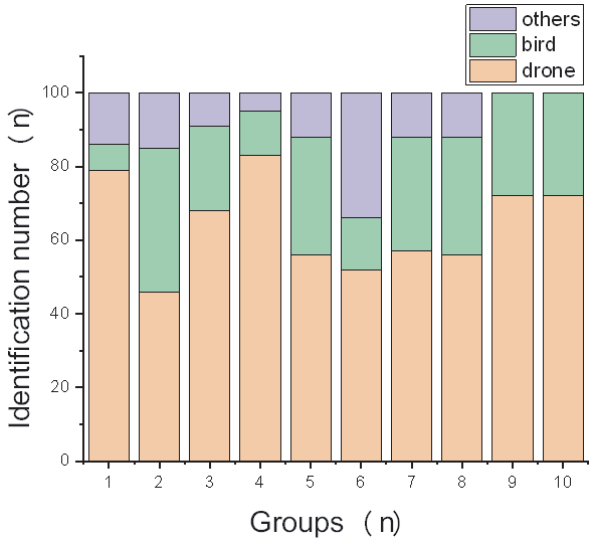

Figure 4. Recognition consequences of a drone's radar echoes when the radar detects the drone. The horizontal axis is group numbers. Every group has 100 sampling frames of radar echoes from drones. The vertical axis describes the recognition time in one group. Blue values represent radar echoes recognized as drones. Red values belong to birds and the green is fresh objects. When the radar detects a drone, birds are a major interference. Others represent objects such as vehicles, people, vortex, ground clutters, or portfolio object.

4. DISCUSSION

There is no doubt that flying birds become the major clutter for radar detecting drones. This will increase the false alarm of the radar system. Therefore, identification of the radar echoes of drones from that of flying birds is a significant demand. The RCS value, signal fluctuation, motion feathers, and micro-Doppler signatures are widely investigated for attempting to identify echoes from birds and drones. When using a low range resolution radar system, typically, the mean velocity component in a spectrogram is due to the motion of a target as a whole, assuming that the body gives the strongest reflection, and the moving parts presents a weaker component [41]. Unfortunately, as our measurement

results, the velocity of flying birds and drones share the same range, such that radial velocity is not discriminative. Radial velocity is not a robust feature since it depends on direction of flight, in addition to the happenstance that the main velocity component comes from wingbeats other than the bird body. Tactical feathers of the tracks are also reported for classifying drones versus non-drones [42], and the result seems to be effective if no account is taken of the lengthy time for establishment of the trajectory. Besides, there is no evident difference in signal function and RCS value between radar echoes from flying birds and drones; thus, empirical thought of the radar operator in our test cannot be applied in artificial discrimination, not to mention automatic target recognition.

Identifiable micro-Doppler signatures cannot be obtained in our radar data. Theoretically, the flapping motion of a bird's wings and the spinning of a drone's propeller blades should register micro-Doppler signatures. There are many studies on those micro-Doppler signatures, but some contradictories still exist. Some studies claim that wings have a negligible effect on bird echo intensity [29], while others attempt to extract amplitude modulation envelope signatures [28] correlated with the flapping pattern of wings [30] to classify bird species [26, 27]. Some investigations believe that the plastic drone blades do not contribute to a significant return [17, 43], but others report that blades give rise to "blade flash" [41], which is a term given to the short impulse of high radar return that is observed in blade signature [16]. Still, there are no visual clues of micro-Doppler for human operators in our Ku-band radar data. Probably, our sampling time in one CPI (i.e., 30 ms) is too short to capture micro-Doppler signatures.

5. CONCLUSIONS

The skies are getting crowded. The near-misses between drones and planes have surged since 2014. Although bird strike hazards are still the major threat to aviation safety, there are many solutions to prevent the potential collision between birds and aircrafts around airports, such as mapping the route of the bird migration to avoid potential collisions and training inspectors to chase away birds. Yet, the flight route of a drone is unpredictable, which makes its detection by the radar system more demanding. Then, the first problem for radar detecting drones is the interference posed by radar echoes from flying birds. In this paper, we find that birds and drones do have similar RCS values because of a similar maximum detectable range, and their radar signals have a similar signal amplitude, fluctuation of time-series, and spectrum structure. The periodic amplitude variations of the echo from a bird modulated by wingbeats are barely seen. Micro-Doppler signatures registered by flapping wings and rotating blades cannot be obtained from radar echoes either. This results in failure in the ability to distinguish the echoes of drones from those of birds by artificial discrimination. Besides, both birds and drones mainly fly at low altitudes. All these factors contribute to flying birds being the major source of interference when radar is detecting and identifying airborne drones. Our recognition results illuminate that the identification probability of airborne drones will be lower due to interference of the radar signal from flying birds. The objective of this paper lies in the support to claims that birds become the jamming of radar detecting drones because of the similarity in RCS and motion pattern, and then the classification between radar echoes from birds and drones can be motivated..

ACKNOWLEDGMENT

The authors thank the data providers who assisted us in the data collection and experimentation. We thank LetPub (www.letpub.com) for its linguistic assistance during the preparation of this manuscript.

REFERENCES

1. Gregory, T. S., Z. T. Tse, and D. Lewis, "Drones: Balancing risk and potential," *Science*, Vol. 347, No. 6228, 1323, 2015.
2. Song, Y., B. Horton, and J. Bayandor, "Investigation of UAS ingestion into high-bypass engines, Part I: Bird vs. drone," *58th AIAA/ASCE/AHS/ASC Structures, Structural Dynamics, and Materials Conference*, American Institute of Aeronautics and Astronautics, Reston, Virginia, 2017.

3. Schroeder, K., Y. Song, B. Horton, and J. Bayandor, "Investigation of UAS ingestion into high-bypass engines, Part II: Parametric drone study," *58th AIAA/ASCE/AHS/ASC Structures, Structural Dynamics, and Materials Conference*, American Institute of Aeronautics and Astronautics, Reston, Virginia, 2017.
4. Gettinger, D. and A. Holland Michel, "Drone sightings and close encountes: An analysis," Center for the Study of the Drone at Bard College, 2015.
5. Nohara, T. J., R. C. Beason, and P. Weber, "Using radar cross-section to enhance situational awareness tools for airport avian radars," *Human-Wildlife Interact.*, Vol. 5, No. 2, 2011.
6. Jahangir, M., C. J. Baker, and G. A. B. T.-R. C. Oswald, "Doppler characteristics of micro-drones with L-Band multibeam staring radar," *IEEE Radar Conference*, 1052–1057, 2017.
7. Troxel, S., B. Echels, W. Pughe, and M. Weber, "Progress report on development of a terminal area bird detection and monitoring system using the ASR-9," *Bird Strike Comm.*, 2002.
8. Molchanov, P., K. Egiazarian, J. Astola, et al., "Classification of small UAVs and birds by micro-Doppler signatures," *European Radar Conference*, 435–444, 2013.
9. Torvik, B., K. E. Olsen, and H. Griffiths, "Classification of birds and UAVs based on radar polarimetry," *IEEE Geosci. Remote Sens. Lett.*, Vol. 13, No. 9, 1305–1309, 2016.
10. Dolbeer, R., S. E. Wright, J. R. Weller, A. L. Anderson, and M. J. Beiger, "Wildlife strikes to civil aircraft in the United States, 1990–2014," *Bird Strikes*, 2015.
11. Fox, A. D. and P. D. L. Beasley, "David Lack and the birth of radar ornithology," *Arch. Nat. Hist.*, Vol. 37, No. 2, 325–332, 2010.
12. Gauthreaux, S., "Radar ornithology and biological conservation," *Auk*, Vol. 120, 266–277, 2009.
13. Moon, J. R., "Effects of birds on radar tracking systems," *IET Conference Publication*, Vol. 490, 300–304, 2002.
14. Harman, S., "A comparison of staring radars with scanning radars for UAV detection: Introducing the Alarm$^{\mathrm{TM}}$staring radar," *IEEER Adar Conference*, 2015.
15. Gustavsson, M., ¤ Andersson, T. Johansson, et al., "Micro-Doppler extraction of a small UAV in a non-line-of-sight urban scenario," *Radar Sensor Technology XXI, International Society for Optics and Photonics*, 2017.
16. Harman, S., "Characteristics of the radar signature of multi-rotor UAVs," *IEEE Radar Conference*, 2016.
17. Stein, K. U., et al., "Numerical RCS and micro-Doppler analysis of a consumer UAV," *SPIE Proceedings [SPIE SPIE Security + Defence — Edinburgh, United Kingdom (Monday, September 26, 2016)] Target and Background Signatures II*, 2016.
18. Ren, J. and X. Jiang, "Regularized 2-D complex-log spectral analysis and subspace reliability analysis of micro-Doppler signature for UAV detection," *Pattern Recognit.*, 2017.
19. Ritchie, M. A., F. Fioranelli, H. Griffiths, et al., "Monostatic and bistatic radar measurements of birds and micro-drone," *IEEE Radar Conference*, 2016.
20. Manfred, B., A. F. Jacob, and S. Lorenz-Peter, "Classification of small UAVs and birds by micro-Doppler signatures," *Int. J. Microw. Wirel. Technol.*, Vol. 6, No. 3–4, 435–444, 2014.
21. Gauthreaux, S. A., "Radar ornithology and biological conservation," *Auk*, Vol. 120, No. 2, 266–277, 2003.
22. Skolnik, M., *Radar Handbook*, McGraw-Hill Education, 2008.
23. Tait, P., *Introduction to Radar Target Recognition*, Institution of Electrical Engineers, 2005.
24. U. S. D. of Transportation and U. S. F. A. Administration, "Airport Avian Radar Systems — Advisory Circular 150/5220-25," 2010.
25. Melnikov, V. M., R. R. Lee, and N. J. Langlieb, "Resonance effects within S-band in echoes from birds," *IEEE Geosci. Remote Sens. Lett.*, Vol. 9, No. 3, 413–416, 2012.
26. Bruderer, B., D. Peter, A. Boldt, and F. Liechti, "Wing-beat characteristics of birds recorded with tracking radar and cine camera," *Ibis (Lond. 1859).*, Vol. 152, No. 2, 272–291, 2010.

27. Zaugg, S., G. Saporta, E. van Loon, H. Schmaljohann, and F. Liechti, "Automatic identification of bird targets with radar via patterns produced by wing flapping," *J. R. Soc. Interface*, Vol. 5, No. 26, 1041–1053, 2008.
28. Bonham, L. L. and L. V. Blake, "Radar echoes from birds and insects," *Sci. Mon.*, Vol. 82, No. 4, 204–209, 1956.
29. Blacksmith, Jr. P. and R. B. Mack, "On measuring the radar cross sections of ducks and chickens," *Proc. IEEE*, Vol. 53, No. 8, 1125, 1965.
30. Konrad, T. G., J. J. Hicks, and E. B. Dobson, "Radar characteristics of birds in flight. Radar tracking of known single birds indicates a characteristic radar signature," *Science*, Vol. 159, No. 3812, 274–280, 1968.
31. Vaughn, C. R., "Birds and insects as radar targets: A review," *Proc. IEEE*, Vol. 73, No. 2, 205–227, 1985.
32. O'Neal, B. J., J. D. Stafford, and R. P. Larkin, "Waterfowl on weather radar: Applying ground-truth to classify and quantify bird movements," *J. F. Ornithol.*, Vol. 81, No. 1, 71–82, 2010.
33. Torvik, B., K. E. Olsen, and H. Griffiths, "K-band radar signature analysis of a flying mallard duck," *14th International Radar Symposium (IRS)*, Vol. 2, 584–591, 2013.
34. Torvik, B., K. E. Olsen, and H. D. Griffiths, "X-band measurements of radar signatures of large sea birds," *International Radar Conference*, 1–6, 2014.
35. Urmy, S. S. and J. D. Warren, "Quantitative ornithology with a commercial marine radar: Standard-target calibration, target detection and tracking, and measurement of echoes from individuals and flocks," *Methods Ecol. Evol.*, Vol. 8, 2016.
36. Van Doren, B. M. and K. G. Horton, "A continental system for forecasting bird migration," *Science*, Vol. 361, No. 6407, 1115–1118, 2018.
37. Ritchie, M., F. Fioranelli, H. Griffiths, and B. B. T.-R. C. Torvik, "Micro-drone RCS analysis," *Radar Conference IEEE*, 452–456, 2016.
38. Pieraccini, M., L. Miccinesi, and N. Rojhani, "RCS measurements and ISAR images of small UAVs," *IEEE Aerosp. Electron. Syst. Mag.*, Vol. 32, No. 9, 28–32, 2017.
39. Farlik, J., M. Kratky, J. Casar, and V. B. T.-I. C, "Radar cross section and detection of small unmanned aerial vehicles," *IEEE International Conference on Mechatronics-Mechatronika*, 452–456, 2017.
40. Nakamura, R. and H. Hadama, "Characteristics of ultra-wideband radar echoes from a drone," *IEICE Commun. Express*, Vol. 6, 2017.
41. Harmanny, R. I. A., J. J. M. De Wit, and G. Prémel Cabic, "Radar micro-Doppler feature extraction using the spectrogram and the cepstrogram," *Euma*, 165–168, 2014.
42. Mohajerin, N., J. Histon, R. Dizaji, and S. L. B. T.-R. C. Waslander, "Feature extraction and radar track classification for detecting UAVs in civillian airspace," *IEEE Radar Conference*, 674–679, 2014.
43. Li, C. and H. Ling, "An investigation on the radar signatures of small consumer drones," *IEEE Antennas Wirel. Propag. Lett.*, Vol. PP, No. 99, 1, 2017.